Technical Notes and Correspondence

A State-Dependent Boundary Layer Design for Sliding Mode Control

Min-Shin Chen, Yean-Ren Hwang, and Masayoshi Tomizuka

***Abstract*—The use of a boundary layer in sliding-mode control has been a common technique to reduce chattering of the control signal. However, different choices of the boundary layer width lead to conflicting effects: a large/small boundary layer width can more/less effectively alleviate the chattering phenomenon, but leads to less/more accurate control results. This note proposes online adjusting the width of the boundary layer based on the state norm for an uncertain linear system. The proposed state-dependent boundary layer design can effectively eliminate chattering while at the same time ensuring *almost perfect* control accuracy.**

***Index Terms*—Boundary layer control, chattering, control accuracy, sliding mode control, variable structure system.**

I. Introduction

Sliding-mode control is known to be robust against parameter uncertainties and external disturbances [1]–[3]. However, for the sliding surface to be *attractive*, a switching function must be used in the control law, which causes chattering of the control signals. In order to reduce chattering, one can introduce a boundary layer [4], [5] around the sliding surface. Inside the boundary layer, the discontinuous switching function is interpolated by a continuous function to avoid discontinuity of the control signals. The width of the boundary layer is normally constant, and the larger the boundary layer width, the smoother the control signal. Even though the boundary layer design alleviates the chattering phenomenon, it no longer drives the system state to the origin, but to a small residual set around the origin. The size of the residual set is determined by the width of the boundary layer: the larger the width of the boundary layer, the larger the size of the residual set. As a consequence, there exists a design conflict between requirements on the smoothness of control signals and on the control accuracy. For smoothness of the control signals, a large boundary layer width is preferred, but for better control accuracy, a small boundary layer width is preferred.

Instead of using a constant width, one can also use a time-varying boundary layer width. In one example [3], the width can be the filtered output of the reference trajectory. In other examples [6], [7], the width is scheduled to decay exponentially starting from some initial value. The decaying-width design is attractive since it ensures the exponential convergence of the system state to zero. The simulation results in [8] also demonstrate that the decaying-width design is effective in maintaining stability in the face of high-frequency unmodeled dynamics. However, in the decaying-width design, the chattering phenomenon inevitably shows up when the width has decayed practically to zero. Another drawback of the decaying width design, which uses a simple "open-loop" tuning of the boundary layer width, is its lack of vigilance to the change of system conditions such as the sudden injection of a disturbance.

A more reasonable approach to the boundary layer design is to schedule the width based on the system state; forming a "closed-loop" tuning of the boundary layer width. In this note, it is proposed that the width of the boundary layer be proportional to the modulus of the system state when controlling an uncertain linear system. The new design can control the system state to *almost* zero with no chattering in the control signals. It is interesting to note the work in [9], where they use a first-order filter to smooth the control signal in a fuzzy sliding mode control design. The filter bandwidth is scheduled to be proportional to the angle between the state vector and the normal vector of the sliding surface. Their design, lacking rigorous mathematical proof, is in spirit similar to the state-dependent boundary layer width design in this note. There are other various approaches proposed to alleviate the chattering problem. Prefiltering of the control signal is one approach. This can be done either by direct insertion of a low-pass filter before the plant [10], or by treating the time derivative of the control input as the design input [11], or as used in the disturbance estimator design in [12]. Another approach is the observer-based sliding mode control [13], which can ease the chattering problem due to unmodeled dynamics by constructing a high-frequency bypass loop. The most common approach is to shape the phase portrait near the sliding surface such that the state velocity vector is almost parallel to the sliding surface. See for example [14]–[16], among which the boundary layer control is recognized to be the most simple and widely used approach.

The remainder of this note is organized as follows. Section II reviews the switching sliding mode control for linear uncertain systems. Section III examines the constant-width and decaying-width boundary layer controls. Section IV introduces the new state-dependent boundary layer control. Finally, Section V gives conclusions. Notice that this note offers a "unified" stability analysis for various boundary layer controls, and this analysis is more concise than those previously proposed. In order not to obscure the development of the control designs, all the proofs of lemmas and theorems are placed in the Appendix.

II. Switching Sliding Mode Control

Consider a *switching* sliding mode control design for a linear system with "matching" uncertainties [17]

$$\dot{x} = Ax + B(u + \Delta Ex + d), \qquad x(0) = x_0 \tag{1}$$

where $x \in R^n$ is the system state, u is a scalar control input, $A \in R^{n\times n}$ and $B \in R^n$ are nominal system matrices satisfying the controllability condition [18], uncertainty ΔE is possibly time-varying, and d an unknown disturbance. The system uncertainties are bounded by two known constants:

$$\|\Delta E\| \le \overline{E} \quad \|d\| \le \overline{D}. \tag{2}$$

Note that one can always perform a state transformation such that the controllable pair (A, B) is in the controller canonical form [18]

$$A = \begin{bmatrix} 0 & 1 & \cdot & \cdot \\ \cdot & 0 & 1 & \cdot \\ \cdot & \cdot & \cdot & \cdot \\ a_1 & \cdot & \cdot & a_n \end{bmatrix} \quad B = \begin{bmatrix} 0 \\ \cdot \\ 0 \\ 1 \end{bmatrix}. \tag{3}$$

Manuscript received July 24, 2001; revised April 3, 2002. Recommended by Associate Editor P. Tomei.

M.-S. Chen is with the Department of Mechanical Engineering, National Taiwan University, Taipei 106, Taiwan, Republic of China (e-mail: mschen@ccms.ntu.edu.tw).

Y.-R. Hwang is with the Department of Mechanical Engineering, National Central University, 310 Chung-Li, Taiwan (e-mail: yhwang@cc.ncu.edu.tw).

M. Tomizuka is with the Department of Mechanical Engineering, University of California, Berkeley, CA 94720-1740 USA (e-mail: tomizuka@me.berkeley.edu).

Digital Object Identifier 10.1109/TAC.2002.803534.

The objective of sliding mode control is to regulate the state x in (1) to zero, and this is achieved by a two-stage control design.

Stage I—Design of the Sliding Variable: First define an augmented state

$$\dot{v} = x_1 \quad \text{or} \quad v = \int_0^t x_1\, d\tau \tag{4}$$

and choose the sliding variable as

$$\begin{aligned} s &= Cx + c_0 v, \qquad C = [c_1, c_2, \ldots, 1] && (5)\\ &= x_n + c_{n-1}x_{n-1} + \cdots + c_1 x_1 + c_0 \int_0^t x_1\, d\tau \\ &= x_1^{(n-1)} + c_{n-1}x_1^{(n-2)} + \cdots + c_1 x_1 + c_0 \int_0^t x_1\, d\tau && (6) \end{aligned}$$

where the coefficients c_is are chosen such that the differential equation (6) is stable (has only left-half plane characteristic roots). The purpose of adding an integral term in (6) is for the special case when the system dimension $n = 1$. Note from (3) and (5) that $CB = 1$.

The differential equations (4) and (6) can be cast into a state-space form

$$\dot{z} = Fz + Gs, \qquad \text{where } z = \begin{bmatrix} \int_0^t x_1\, d\tau \\ x_1 \\ \cdot \\ \cdot \\ x_{n-1} \end{bmatrix} \in R^n \tag{7}$$

and matrices F and G are in controller canonical form:

$$F = \begin{bmatrix} 0 & 1 & \cdot & \cdot \\ \cdot & 0 & 1 & \cdot \\ \cdot & \cdot & \cdot & \cdot \\ -c_0 & \cdot & \cdot & -c_{n-1} \end{bmatrix} \in R^{n\times n} \quad G = \begin{bmatrix} 0 \\ \cdot \\ 0 \\ 1 \end{bmatrix} \in R^n. \tag{8}$$

Since the differential equation (6) is stable by the choice of the coefficients c_i's, the matrix F in (7) is stable.

Several results regarding (7) that will be repeatedly used in later sections are listed below. Firstly, given the stable matrix F in (8), there exist positive constants m and α such that

$$\left\| e^{F(t-\tau)} \right\| \le m e^{-\alpha(t-\tau)} \qquad \forall\, t \ge \tau \tag{9}$$

where α is treated as a control design parameter since its value is determined by the choices of $c_i's$ in (6). Second, given any positive constant $\sigma \ge -\mathrm{Re}[\lambda_i(F)] > 0$ for all i, where $\mathrm{Re}[\lambda_i(F)]$ denotes the real part of eigenvalues of F, there exists a positive definite matrix $P \in R^{n\times n}$ satisfying the following Lyapunov inequality:

$$(-F-\sigma I)^T P + P(-F-\sigma I) \le 0, \qquad \sigma \ge -\mathrm{Re}[\lambda_i(F)] > 0 \qquad \forall\, i. \tag{10}$$

Finally, from linear system theory [18], the state in (7) satisfies

$$z(t) = e^{Ft} z(0) + \int_0^t e^{F(t-\tau)} G s(\tau)\, d\tau. \tag{11}$$

Stage II—Design of the Control Input: The *stable* state space equation (7) suggests that if the sliding variable s can be driven to zero by some control design, the state z will decay to zero. Therefore, one chooses the following "switching" sliding mode control to drive s to zero:

$$u = -\sigma s - c_0 x_1 - CAx - \rho(x) f_0(s) \tag{12}$$

where $\sigma > 0$, s is the sliding variable, $\rho(x) = \rho_0(\overline{E}\|x\| + \overline{D})$, $\rho_0 > 1$, with $\overline{E}$ and $\overline{D}$ given by (2), and $f_0(s)$ a switching function

$$f_0(s) = sgn(s) = \begin{cases} 1, & s > 0 \\ -1, & s < 0. \end{cases} \tag{13}$$

Lemma 1 [3]: If the switching sliding-mode control (12) is applied to the uncertain system (1), there exists a finite time T_0 such that $|s(t)| = 0$ for all $t > T_0$.

Once $s(t)$ becomes zero according to Lemma 1, the state z in (7) starts to decay exponentially, and so does the state x in (1).

Theorem 1 [3]: If the switching sliding mode control (12) is applied to the uncertain system (1), the system state x will converge to zero exponentially.

III. Constant/Decaying-Width Boundary Layer Control

In practical implementation of the switching control (12), the imperfect switching of the discontinuous function $f_0(s) = sgn(s)$ causes the control signal to chatter [3]. Such chattering may bring damage to the actuator or excite high-frequency unmodeled dynamics. To alleviate the problem, a boundary layer around the sliding surface $s = 0$ is suggested to smooth the control signal. The result is the so-called *boundary layer control*

$$u = -\sigma s - c_0 x_1 - CAx - \rho(x) f_1(s) \tag{14}$$

where the discontinuous function $f_0(s) = sgn(s)$ in the switching control (12) is now replaced by a continuous function

$$f_1(s) = \frac{s}{|s| + \epsilon_0 e^{-\pi t}}, \qquad \sigma > \pi \ge 0,\ \epsilon_0 > 0 \tag{15}$$

in which $\epsilon_0 e^{-\pi t}$ is the width of the boundary layer, which decays exponentially to zero when $\pi \ne 0$, and remains constant when $\pi = 0$.

Lemma 2: If the boundary layer control (14) is applied to (1), then

$$|s(t)| \le \eta_0 e^{-\pi t} + |s(0)| e^{-\sigma t}, \qquad \eta_0 = \frac{\epsilon_0}{\rho_0 - 1}. \tag{16}$$

If π chosen to be positive, it is a decaying-width boundary layer design. In this case, *exponential* stability of the controlled system is guaranteed by the control (14).

Theorem 2: If the decaying-width boundary layer control (14) ($\pi > 0$) is applied to the uncertain system (1), the system state x will converge to zero exponentially.

If π is chosen to be zero, it is a constant-width boundary layer design. In this case, the so-called *practical* stability is guaranteed in the sense that given any small neighborhood of the origin, there always exist control design parameters in (14) such that the state will eventually be trapped in the specified neighborhood.

Theorem 3: If the constant-width boundary layer control (14) ($\pi = 0$) is applied to the uncertain system (1), the system state x will asymptotically approach a residual set around the origin, with the size of the residual set proportional to $\epsilon_0/(\rho_0 - 1)$, $\rho_0 > 1$.

The following simulation examples demonstrate the effects of using different values of ϵ_0 and π in the boundary layer control (14).

Example 1 Constant Boundary Layer Width: Consider a disturbance rejection problem for (1) with

$$A = \begin{bmatrix} 0 & 1 \\ 0 & 0 \end{bmatrix} \quad B = \begin{bmatrix} 0 \\ 1 \end{bmatrix}$$

the disturbance $d(t) = \sin(t)$, system uncertainty $\Delta E = 0$, and $x^T(0) = [5, -2]$. The constant-width boundary layer control (14) is applied to the system with $\pi = 0$, $\rho_0 = 1.5$, $\sigma = 2$, $\overline{E} = 0$, $\overline{D} = 1$ and $c_0 = 1$, $c_1 = 2$, $c_2 = 1$ in (6). Two computer simulations are tested: one with a small constant boundary layer width $\epsilon_0 = 0.001$,

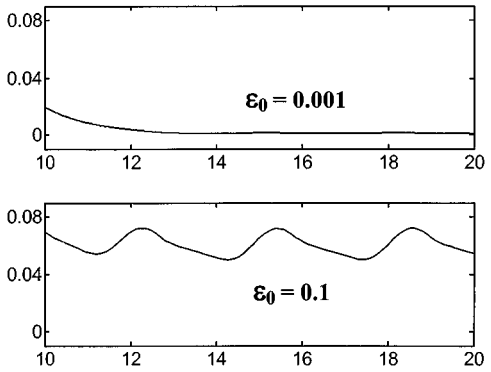

Fig. 1. Time history of state norm $\|x(t)\|$.

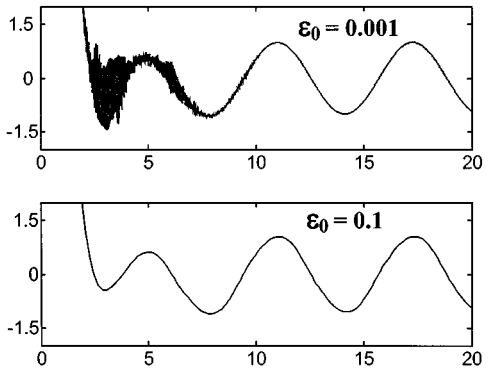

Fig. 2. Time history of control signal $u(t)$.

and the other with a large width $\epsilon_0 = 0.1$. Fig. 1 plots $\|x(t)\|$ versus t for $t \in [10, 20]$, which clearly shows that the control with a smaller boundary layer width (the upper plot) results in better control accuracy, while the control with a larger width (the lower plot) results in much worse control accuracy. On the other hand, one can see from Fig. 2 that the use of a smaller boundary layer width (the upper plot) causes severe chattering in the control signal during the transient (say $t \in [2, 8]$), while the use of a larger width (the lower plot) can effectively alleviate the chattering phenomenon.

Example 2 Decaying Boundary Layer Width: The same system as in Example 1 is simulated by the control (14) with $\pi = 0.1$, $\epsilon_0 = 0.1$, and all other design parameters the same as in Example 1. In this case, the boundary layer width decays exponentially because $\pi > 0$. At $t = 50$ second, the system is subject to an impulsive type disturbance, which brings the state to $x^T(50^+) = [3, 4]$. When the control drives the state close to the sliding surface again, chattering shows up as shown in the lower plot of Fig. 3 ($t \in [40, 60]$), and this is because the boundary layer width has decayed practically to zero. This example reflects that the decaying-width design lacks the ability to respond to the change of system conditions.

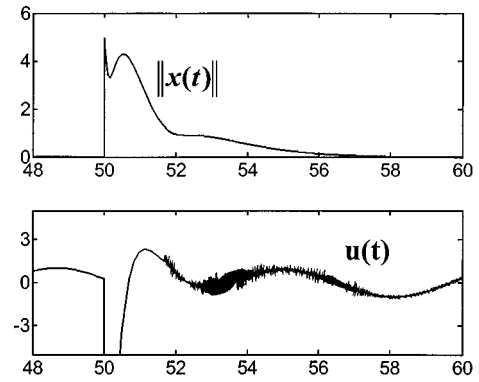

Fig. 3. Control with decaying width $\epsilon_0 = 0.1e^{-0.1t}$.

IV. State-Dependent Boundary Layer Control

As is demonstrated by the first simulation example in Section III, the constant-width boundary layer design can reduce chattering of the control signals, but it decreases the control accuracy. The compromise between the smoothness of control signals and the accuracy of control results is dictated by the choice of the boundary layer width [ϵ_0 in (15)]. A solution to this design conflict is revealed by a careful examination of Figs. 1 and 2, which shows that for the control with a small boundary layer width, chattering occurs only during the transient stage when the system state is far from the origin. When the state becomes closer and closer to the origin, the chattering phenomenon gradually disappears even though the boundary layer width is very small. This observation suggests that when $\|x\|$ is large, one should use a large boundary layer width to avoid chattering, and when $\|x\|$ is small, use a small boundary layer width to achieve good control accuracy. Therefore, this note proposes that the boundary layer width be proportional to the modulus of the system state. Such a design automatically adjusts the boundary layer width based on the system condition, and will be more capable of dealing with unexpected situations such as the one seen in the simulation Example 2.

The aforementioned reasoning leads to the following *state-dependent boundary layer control*

$$u = -\sigma s - c_0 x_1 - CAx - \rho(x) f_2(s) + \eta_1^2 G^T P z + \eta_0 \eta_1 G^T P e_z \tag{17}$$

where P is as in (10), G as in (8), z the state in (7), $\eta_1 = \epsilon_1/(\rho_0 - 1) > 0$, $\eta_0 = \epsilon_0/(\rho_0 - 1) > 0$, $e_z = z/\|z\|_p$ and

$$f_2(s) = \frac{s}{|s| + \epsilon_1 \|z\|_p + \epsilon_0}, \qquad \|z\|_p \triangleq \sqrt{z^T P z} \tag{18}$$

in which $\epsilon_1 > 0$ and $1 \gg \epsilon_0 > 0$. Since $\epsilon_0 \approx 0$, the boundary layer width in (18) is approximately proportional to the state norm $\|z\|_p$. The reason for adding this small ϵ_0 in the boundary layer width is to prevent $f_2(\cdot)$ from degenerating into the discontinuous $sign(\cdot)$ function when the state z has decayed practically to zero. Note that there are two extra feedback terms (the last two terms) in the new control (17), which serve to ensure that the inequality (19) in Lemma 3 holds.

Lemma 3: If the new boundary layer control (17) is applied to the uncertain system (1), the sliding variable s will be bounded by, for all $t > 0$

$$|s(t)| \le \eta_1 \|z(t)\|_p + \eta_0 + |s(0)| e^{-\sigma t}$$
$$\eta_1 = \epsilon_1/(\rho_0 - 1),\ \eta_0 = \epsilon_0/(\rho_0 - 1). \tag{19}$$

Lemma 4 (Bellman–Gronwall's Lemma) [18]: If a continuous function $f(t) \ge 0$ satisfies

$$f(t) \le b(t) + \int_{t_0}^{t} k(\tau) f(\tau)\, d\tau \qquad \forall\, t \ge t_0$$

where $b(t) \ge 0$ and $k(t) \ge 0$ are continuous and nonnegative for all $t \ge t_0$, then

$$f(t) \le b(t) + \int_{t_0}^{t} b(\tau) k(\tau) \exp\left(\int_{\tau}^{t} k(v)\, dv \right) d\tau \qquad \forall\, t \ge t_0.$$

Substituting the result of Lemma 3 into (11), and using Bellman–Gronwall's Lemma, one can establish the following stability result for the state-dependent boundary layer control.

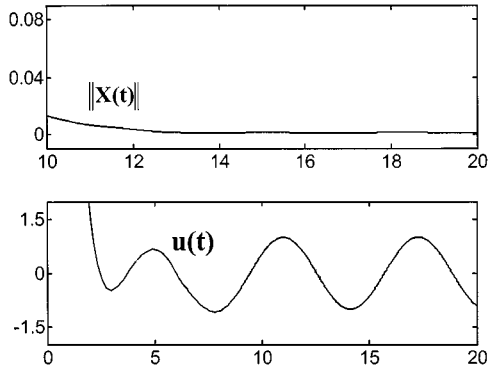

Fig. 4. State-dependent boundary layer control with $\epsilon_0 = 0.001$ and $\epsilon_0 = 0.1$.

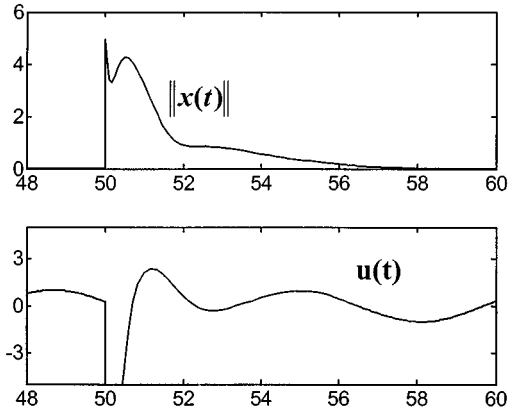

Fig. 5. Control with state-dependent width.

Theorem 4: Consider the uncertain system (1) and the state-dependent boundary layer control (17). If the control design parameters are chosen to satisfy

$$\epsilon_1 > 0, \qquad 1 \gg \epsilon_0 > 0, \qquad \rho_0 > 1$$
$$\sigma \geq -\mathrm{Re}[\lambda_i(F)] > 0, \qquad \alpha > \frac{\epsilon_1}{\rho_0 - 1}\, m \sqrt{\overline{\sigma}_p} \tag{20}$$

where α and m are as in (9), $\overline{\sigma}_p$ is the maximum singular value of P in (10), F is given by (8), then the system state x will asymptotically approach a residual set around the origin, with the size of the residual set proportional to ϵ_0.

The following example verifies the new boundary layer design.

Example 3 State-Dependent Boundary Layer Width: Consider the same problem as in Example 1. A computer simulation with the new state-dependent boundary layer control (17) is performed with $\epsilon_1 = 0.1$, $\epsilon_0 = 0.001$, and all other design parameters the same as in Example 1. The upper plot in Fig. 4 shows $\|x(t)\|$ versus time t for $t \in [10, 20]$. As can be seen that the state-dependent boundary layer control achieves the same control accuracy as the previous control (14) with a small constant boundary layer width (the upper plot in Fig. 1). Furthermore, the lower plot in Fig. 4 shows that the proposed state-dependent boundary layer control (17) successfully avoids chattering of the control signal.

In the second simulation, at $t = 50$ s, similar to the experiment done in Example 2, the system state is suddenly transferred to $x^T(50^+) = [3, 4]$ by an impulse disturbance, and the result for $t \in [40, 60]$ is shown in Fig. 5. It is seen from the lower plot that the proposed new design successfully avoids the chattering problem in the decaying-width design in Fig. 3, and this is because the new design can respond immediately to the change of system conditions.

V. Conclusion

This paper proposes a new boundary layer design that resolves the long-existent design dilemma in sliding-mode control between the requirements of control accuracy and control signal smoothness. It is interesting to extend this new design to nonlinear system control [19], [20].

Finally, it is reminded that smoothing of the control signal in the boundary layer design may be accomplished by continuous interpolation functions different from $f_2(\cdot)$ in (17). For example, another commonly used interpolation function is the *saturation* function $h_1(s) = s$ if $|s| \leq \epsilon_0$ and $h_1(s) = sgn(s)$ otherwise. For the new state-dependent boundary layer design proposed in this note, the $h_1(\cdot)$ function should be modified to $h_2(s) = s/(\epsilon_1 \|z\|_p + \epsilon_0)$ if $|s| \leq \epsilon_1 \|z\|_p + \epsilon_0$ and $h_2(s) = sgn(s/(\epsilon_1 \|z\|_p + \epsilon_0))$, otherwise.

Appendix

Proof for Lemma 2: Define a region Ω_0 in the extended state space by

$$\Omega_0 = \left\{ x_v \triangleq \begin{bmatrix} v \\ x \end{bmatrix} \in R^{n+1} \colon |s| \leq \eta_0 e^{-\pi t},\ \eta_0 = \epsilon_0/(\rho_0 - 1) \right\}.$$

Check the time derivative of $(s^2 - \eta_0^2 e^{-2\pi t})$ along the closed-loop trajectory (1) and (14)

$$\frac{d}{dt}(s^2 - \eta_0^2 e^{-2\pi t}) \leq -2\sigma s^2 + 2\pi \eta_0^2 e^{-2\pi t} - \rho_0 |s| \left(\overline{E}\, \|x\| + \overline{D} \right) \left(\frac{|s|}{|s| + \epsilon_0 e^{-\pi t}} - \frac{1}{\rho_0} \right).$$

Since the term in the rightmost parenthesis is greater than zero for $|s| > \eta_0 e^{-\pi t}$ (or $x_v \notin \Omega_0$), one has, using $\pi < \sigma$

$$\frac{d}{dt}(s^2 - \eta_0^2 e^{-2\pi t}) \leq -2\sigma (s^2 - \eta_0^2 e^{-2\pi t}) \qquad \forall\, x_v \notin \Omega_0. \tag{A1}$$

Integrating the inequality suggests that Ω_0 is *attractive* since

$$s^2(t) - \eta_0^2 e^{-2\pi t} \leq (s^2(0) - \eta_0^2) e^{-2\sigma t} \tag{A2}$$

where t is any time before the extended system state x_v enters the region Ω_0. One can further deduce from (A2) that $s^2(t) \leq \eta_0^2 e^{-2\pi t} + s^2(0) e^{-2\sigma t} \leq (\eta_0 e^{-\pi t} + |s(0)| e^{-\sigma t})^2$. Taking the square root of the inequality proves that (16) holds for any time before x_v enters the region Ω_0.

Once the system state x_v has entered Ω_0, which is *invariant* due to the definition of Ω_0 and (A1), it will remain in Ω_0 forever. If $x_v(t) \in \Omega_0$, one has, by definition, $|s(t)| \leq \eta_0 e^{-\pi t} \leq \eta_0 e^{-\pi t} + |s(0)| e^{-\sigma t}$. Hence, (16) holds both before and after x_v enters Ω_0. □

Proof for Theorem 2: Substituting the result of Lemma 2 with $\pi > 0$ into (11), one can derive that

$$\|z(t)\| \leq m \left(\|z(0)\| - \frac{\eta_0}{\alpha - \pi} - \frac{|s_0|}{\alpha - \sigma} \right) e^{-\alpha t} + \frac{m|s(0)|}{\alpha - \sigma} e^{-\sigma t} + \frac{m\eta_0}{\alpha - \pi} e^{-\pi t}.$$

Hence, $z(t)$ decays to zero exponentially, and so does $x(t)$ following the definitions of $z(t)$ in (7) and $s(t)$ in (6). □

Proof for Theorem 3: Substituting the result of Lemma 2 with $\pi = 0$ into (11), one can derive, using (9) and $\|G\| = 1$, that

$$\|z(t)\| \leq m \left(\|z(0)\| - \frac{\eta_0}{\alpha} - \frac{|s_0|}{\alpha - \sigma} \right) e^{-\alpha t} + \frac{m|s(0)|}{\alpha - \sigma} e^{-\sigma t} + \frac{m}{\alpha} \eta_0.$$

Therefore

$$\lim_{t \to \infty} \|z(t)\| \leq \frac{m}{\alpha} \eta_0. \tag{B1}$$

By definitions of s in (5) and z in (7), $x_n = s - \overline{C} z$, where $\overline{C} = [c_0, \ldots, c_{n-1}]$. Hence, $|x_n| \leq |s| + \|\overline{C}\| \cdot \|z\|$. Combining

the previous inequality with $\|x\| \leq \|z\| + |x_n|$, one obtains $\|x\| \leq |s| + (1 + \|\overline{C}\|)\|z\|$. Finally, using (16) and (B1), one concludes that $\lim_{t\to\infty}\|x\| \leq [1 + (1 + \|\overline{C}\|)m/\alpha] \cdot \eta_0$, where $\eta_0 = \epsilon_0/(\rho_0 - 1)$, and α, ρ_0 and ϵ_0 are control design parameters in the control law. □

Proof for Lemma 3: The proof is very much similar to that of Lemma 2; hence only the first few steps are shown as follows. Define a region Ω_z in the extended state space by

$$\Omega_z = \left\{ x_v \triangleq \begin{bmatrix} v \\ x \end{bmatrix} \in R^{n+1} \colon |s| \leq \eta_1 \|z\|_p + \eta_0, \quad \eta_1 = \frac{\epsilon_1}{\rho_0 - 1},\ \eta_0 = \frac{\epsilon_0}{\rho_0 - 1} \right\}.$$

Check the time derivative of the following quantity along the trajectory (1) and (17):

$$\begin{aligned} &\frac{d}{dt}\left[s^2 - (\eta_1\|z\|_p + \eta_0)^2\right] \\ &\quad = 2s\dot{s} - \left(\eta_1^2 \frac{d\|z\|_p^2}{dt} + \eta_1\eta_0 \frac{1}{\|z\|_p}\frac{d\|z\|_p^2}{dt}\right) \\ &\quad \leq -2\sigma[s^2 - (\eta_1\|z\|_p + \eta_0)^2] - 2\rho_0|s|\left(\overline{E}\,\|x\| + \overline{D}\,\right) \\ &\qquad \cdot \left(\frac{|s|}{|s| + \epsilon_1\|z\|_p + \epsilon_0} - \frac{1}{\rho_0}\right) \\ &\quad \leq -2\sigma[s^2 - (\eta_1\|z\|_p + \eta_0)^2] \qquad \forall\, x_v \notin \Omega_z \end{aligned}$$

where one has purposely added two terms $2\sigma(\eta_1\eta_0\|z\| + \eta_0^2)$ and used (2), (10) and (14) to derive the first inequality. The remainder of this proof follows exactly the same argument as in Lemma 2, and is omitted here. □

Proof for Theorem 4: Substituting (19) into (11), and using (9), $\|G\| = 1$ and $\|z\|_p \leq \sqrt{\overline{\sigma}_p}\|z\|$, one can derive

$$\|z(t)\|_p \leq \sqrt{\overline{\sigma}_p}\, m e^{-\alpha t}\|z(0)\| + \int_0^t \sqrt{\overline{\sigma}_p}\, m e^{-\alpha(t-\tau)} \cdot(\eta_1\|z(\tau)\|_p + \eta_0 + |s(0)|e^{-\sigma\tau})\, d\tau. \quad \text{(C1)}$$

Let $q(t) = e^{\alpha t}(\eta_1\|z(t)\|_p + \eta_0 + |s(0)|e^{-\sigma t})$. The following can be deduced from (C1):

$$q(t) \leq \left(\eta_1 m\sqrt{\overline{\sigma}_p}\,\|z(0)\| + \eta_0 e^{\alpha t} + |s(0)|e^{-(\sigma-\alpha)t}\right) + \int_0^t \eta_1 m\sqrt{\overline{\sigma}_p}\, q(\tau)\, d\tau.$$

Applying the Bellman–Gronwall Lemma to the aforementioned inequality yields

$$\begin{aligned} q(t) \leq\ & \eta_1 m\sqrt{\overline{\sigma}_p}\,\|z(0)\| e^{\eta_1 m\sqrt{\overline{\sigma}_p}\, t} + \eta_0 e^{\alpha t} \\ &+ |s(0)|e^{(\alpha-\sigma)t} + \frac{\eta_1 m\sqrt{\overline{\sigma}_p}\,\eta_0}{\alpha - \eta_1 m\sqrt{\overline{\sigma}_p}}\left[e^{\alpha t} - e^{\eta_1 m\sqrt{\overline{\sigma}_p}\, t}\right] \\ &+ \frac{\eta_1 m\sqrt{\overline{\sigma}_p}\,|s(0)|}{\alpha - \eta_1 m\sqrt{\overline{\sigma}_p} - \sigma}\left[e^{(\alpha-\sigma)t} - e^{\eta_1 m\sqrt{\overline{\sigma}_p}\, t}\right]. \end{aligned}$$

Recalling the definition of $q(t)$, one can deduce that $\|z\|_p$ satisfies

$$\begin{aligned} \|z(t)\|_p \leq\ & m\sqrt{\overline{\sigma}_p}\,\|z(0)\| e^{-(\alpha - \eta_1 m\sqrt{\overline{\sigma}_p})t} \\ &+ \frac{m\sqrt{\overline{\sigma}_p}\,\eta_0}{\alpha - \eta_1 m\sqrt{\overline{\sigma}_p}}\left[1 - e^{-(\alpha - \eta_1 m\sqrt{\overline{\sigma}_p})t}\right] \\ &+ \frac{m\sqrt{\overline{\sigma}_p}\,|s(0)|}{(\alpha - \eta_1 m\sqrt{\overline{\sigma}_p} - \sigma)}\left[e^{-\sigma t} - e^{-(\alpha - \eta_1 m\sqrt{\overline{\sigma}_p})t}\right]. \end{aligned}$$

Since $\alpha > \eta_1 m\sqrt{\overline{\sigma}_p}$ by (20), one obtains

$$\lim_{t\to\infty}\|z(t)\|_p \leq \beta_0\epsilon_0, \qquad \beta_0 = \frac{m\sqrt{\overline{\sigma}_p}}{\alpha - \eta_1 m\sqrt{\overline{\sigma}_p}}\left(\frac{1}{\rho_0 - 1}\right).$$

Finally, following the same procedure as in the proof of Theorem 2, one can show that

$$\lim_{t\to\infty}\|x(t)\| \leq \beta_1\epsilon_0, \qquad \beta_1 = \frac{1}{\rho_0 - 1} + \left(\frac{1 + \|\overline{C}\|}{\sqrt{\underline{\sigma}_p}} + \eta_1\right)\beta_0.$$

Therefore, one concludes that x asymptotically approaches a residual set around the origin, with the size of the residual set proportional to ϵ_0. □

REFERENCES

[1] V. I. Utkin, "Variable structure systems with sliding modes," *IEEE Trans. Automat. Contr.*, vol. AC-22, pp. 212–222, 1977.

[2] J. Y. Hung, W. B. Gao, and J. C. Hung, "Variable structure control: A survey," *IEEE Trans. Ind. Electron.*, vol. 40, pp. 2–22, Feb. 1993.

[3] J. J. E. Slotine and W. Li, *Applied Nonlinear Control*. Upper Saddle River, NJ: Prentice-Hall, 1991.

[4] J. J. E. Slotine and S. S. Sastry, "Tracking control of nonlinear systems using sliding surfaces with application to robot manipulator," *Int. J. Control*, vol. 38, no. 2, pp. 931–938, 1983.

[5] J. A. Burton and A. S. I. Zinober, "Continuous approximation of variable structure control," *Int. J. Syst. Sci.*, vol. 17, no. 6, pp. 875–885, 1986.

[6] M. J. Corless and G. Leitmann, "Adaptive control for systems containing uncertain functions and uncertain functions with uncertain bounds," *J. Optim. Theory Appl.*, vol. 41, pp. 155–168, 1983.

[7] Z. Qu, "Global stabilization of nonlinear systems with a class of unmatched uncertainties," *Syst. Control Lett.*, vol. 18, pp. 301–307, 1992.

[8] H. Yu, L. D. Seneviratne, and S. W. E. Earles, "Exponentially stable robust control law for robot manipulators," *IEE Proc. Control Theory Appl.*, vol. 141, pp. 389–395, 1994.

[9] Y. R. Hwang and M. Tomizuka, "Fuzzy smoothing algorithms for variable structure systems," *IEEE Trans. Fuzzy Syst.*, vol. 2, pp. 277–284, Nov. 1994.

[10] A. S. Zinober, O. M. E. EI-Ghezawi, and S. A. Billings, "Multivariable variable-structure adaptive model-folling control systems," *Proc. Inst. Elect. Eng.*, vol. 129, pp. 6–12, 1982.

[11] G. Bartolini, "Chattering phenomena in discontinuous control systems," *Int. J. Syst. Sci.*, vol. 20, pp. 2471–2481, 1989.

[12] K. D. Young and S. V. Drakunov, "Discontinuous frequency shaping compensation for uncertain dynamic systems," in *Proc. 12th IFAC World Congr.*, Sydney, Australia, 1993, pp. 39–42.

[13] A. G. Bondarev, S. A. Bondarev, N. E. Kostyleva, and V. I. Utkin, "Sliding modes in systems with asymptotic state observers," *Automat. Rem. Control*, pp. 679–684, 1985.

[14] M. D. Espana, R. S. Orgega, and J. J. Espino, "Variable structure systems with chattering reduction: A microprocessor based design," *Automatica*, vol. 20, pp. 133–134, 1984.

[15] F. J. Chang, S. H. Twu, and S. Chang, "Adaptive chattering alleviation of variable structure systems control," *Proc. Inst. Elect. Eng.*, vol. 137, pp. 31–39, 1990.

[16] V. I. Utkin, "Variable structure systems and sliding mode—State of the art assessment," in *Variable Structure Control for Robotics and Aerospace Applications*, K. K. D. Young, Ed. New York: Elsevier Science, 1993.

[17] B. Drazenovic, "The invariance condition in variable structure systems," *Automatica*, vol. 5, no. 3, pp. 287–295, 1969.

[18] F. Callier and C. A. Desoer, *Linear System Theory*. New York: Springer-Verlag, 1991.

[19] M. J. Corless and G. Leitmann, "Continuous state feedback guaranteeing uniform ultimate boundedness for uncertain dynamic systems," *IEEE Trans. Automat. Contr.*, vol. AC-26, pp. 1139–1143, 1981.

[20] S. Sastry, *Nonlinear Systems, Analysis, Stability, and Control*. New York: Springer-Verlag, 1999.